



Contents lists available at ScienceDirect

## Computer Communications

journal homepage: [www.elsevier.com/locate/comcom](http://www.elsevier.com/locate/comcom)

# An energy efficient framework for user association and power allocation in HetNets with interference and rate-loss constraints

Rahul Thakur\*, Rajkarn Singh, C. Siva Ram Murthy

Department of Computer Science and Engineering, Indian Institute of Technology Madras, 600036, India

## ARTICLE INFO

### Article history:

Received 21 February 2016

Revised 29 June 2016

Accepted 19 August 2016

Available online xxx

### Keywords:

Cellular networks

Femtocell

Cell biasing

Interference

Rate loss

Energy efficiency

Performance evaluation

## ABSTRACT

Dense deployment of femtocells has proved to be an effective solution to handle increasing demands of indoor mobile data. A femtocell not only helps reducing operational and capital expenditure but also improves the energy efficiency of the network. Femtocells are able to increase spectrum efficiency by manyfold by reusing the available spectrum for indoor users. However, it has been seen that traditional cell selection schemes limit the user count under femtocell. Additionally, dense deployment of femtocells comes with the cost of increased interference to the neighbouring femtocell and macrocell users. In this paper, we first analyse various cell selection schemes to improve user association and resource utilization in femtocells. Then, we focus on improving energy efficiency and throughput of femtocell based cellular networks. For this, we formulate an optimization problem that efficiently reuses macrocell spectrum in femtocells with power control while satisfying macrocell users' interference and rate-loss constraints.

© 2016 Elsevier B.V. All rights reserved.

## 1. Introduction

Advancements in mobile communications have reached to an extent where users can expect ubiquitous connectivity on their mobile devices. This has led to a sudden increase in data demands from mobile users. Interestingly, it has been observed that a major fraction of data demands (nearly 80%) originates from indoor nomadic users [1]. In the last couple of years, we have seen an exponential increase in mobile data demands, especially due to the development of mobile platforms such as Android and Windows, and applications such as Gmail and Facebook which always remain connected to the Internet. With the availability of cheap, low-cost smartphones and tablets, these demands will continue to increase in coming future. According to the forecasts made in [2], an increase in mobile data traffic by 20 times is expected by the end of 2018.

To handle ever-increasing mobile data demands, it is imperative to significantly improve the capacity of wireless networks. Various solutions have been proposed over the years which lead to doubling up the wireless capacity every 30 months over the last 104 years. This results in an approximately millionfold increase in capacity of wireless networks since 1957 [3]. Breaking

down these gains, the use of next-generation cellular technologies (LTE-A, WiMax) combined with better modulation and coding techniques resulted in a  $5 \times$  improvement in wireless capacity. However, these gains are limited by the received signal strength at mobile users and hence not always achievable. Another solution is the use of wider spectrum which has resulted in an approximate  $25 \times$  improvement in wireless capacity. Deployment of small cell base stations is the simplest and the most feasible solution to improve the capacity of wireless networks. It has resulted in a  $1600 \times$  gain in wireless capacity through frequency reuse with power control. However, additional base station deployment burdens operators with extra capital expenditure. Additionally, these base stations consume a significant amount of energy for their operation leading to a higher operational expenditure [4].

To handle indoor cellular data demands without significantly increasing operators' expenditure, use of femtocells has been suggested [3]. Femtocell or Femto Access Point (FAP) is a small, low cost, low power cellular base station deployed inside users' homes to provide better cellular coverage. The inherent low transmission power capabilities of femtocells allow efficient reuse of available spectrum without significantly increasing interference to nearby users. Additionally, indoor users get benefited by stronger signal quality, higher bandwidth, and better battery life because of the reduced uplink transmission power [5].

Since placement locations of femtocells are random, traditional network planning techniques fail to circumvent the interference introduced by them to primary macrocell and neighbouring

\* Corresponding author.

E-mail addresses: [rahulthakur.ms@gmail.com](mailto:rahulthakur.ms@gmail.com) (R. Thakur), [raj555karan@gmail.com](mailto:raj555karan@gmail.com) (R. Singh), [murthy@iitm.ac.in](mailto:murthy@iitm.ac.in) (C.S.R. Murthy).

femtocell users. The best way to eliminate interference in this scenario is to use orthogonal subchannels among macrocell and femtocell users. However, this diminishes the available spectrum to users in both tiers. Another approach is to allow femtocells to control their transmit power to minimize interference. However, lowering transmit power affects femtocell coverage and limits user association in them. This further reduces the resource utilization of already under-utilised femtocells. In current cellular network deployments, the utilization of resources (such as spectrum and transmit power) in macrocells is very high, specially during peak hours when unavailability of resources even leads to call blocking [6]. On the other hand, femtocell utilization is found to be significantly low (about 30%) owing to their low transmit power and coverage radius [7,8]. Hence, to reap the gains of femtocell deployments, offloading of users from macrocell to femtocells is necessary. User offloading schemes help to free up expensive macrocell resources allocated to the offloaded users earlier, thereby increasing spectrum efficiency as well as energy efficiency.

In order to improve user association in femtocell, various solutions have been proposed in the literature. Recently, the concept of cell biasing for femtocells has been introduced in [5,9,10]. Cell biasing attempts to offload users from macrocells to smaller cells by modifying cell selection/handover criteria. The authors of [11] derived a closed form expression to calculate range expansion bias for both uplink and downlink for picocells while mitigating inter-cell interference. Performance analysis of Heterogeneous Networks (HetNets) for multiple small cell densities, bias values, and resource partitioning strategies have been discussed extensively in [12]. User association based on expected bitrate is recently suggested in [13]. This scheme shows quite an improvement in system throughput compared to reference signal and cell biasing based association. Our previous work in [14] suggested an enhancement to this expected bitrate cell selection scheme, further improving system throughput and energy efficiency. For better load balancing, various techniques have been proposed in the literature. Use of transmission power control is the preferred technique for range expansion and load balancing [15]. Authors in [16] proposed a heuristic based approach for inter-femtocell coordination while maintaining fairness. In [17] and [18], authors demonstrate that fractional transmission power control provides improved performance to cell edge users. Work in [19] adjusts femtocell transmission power by a decentralized algorithm so as to balance user load among co-located femtocells.

In this paper, for the first time a framework for joint user association and power allocation for femtocell based cellular network is proposed. The motivation behind studying both of these problems together comes from the fact that the problem of resource allocation in HetNets is immensely coupled with the problem of cell selection. A cell selection scheme may result in an unbalanced user association in HetNets. Additionally, this may result in severe co-channel interference if wireless resources such as bandwidth and transmit power are not carefully partitioned among users of different base stations. Hence, for optimal network performance, a centralised user association and power allocation framework is necessary which can jointly assign users to base stations and control interference on them using transmission power control [20]. The contributions of our work are twofold: (i) we propose the use of an energy efficient, load-conscious cell selection scheme for user offloading to femtocells and (ii) to further improve spectrum efficiency, we suggest a power control based subchannel reuse scheme for femtocell downlink. First, we examine the offloading benefits of different cell selection schemes for femtocell network and focus on evaluating network performance in terms of throughput and energy efficiency. Four existing cell selection schemes are used to offload users from macrocell to femtocells. To protect channel quality of these newly offloaded femtocell users, we suggest exclusive use

of a subset of subchannels for them. Our aim is to improve energy efficiency of the network, which is achieved by reducing energy consumption as well as maximising system throughput. First, to reduce energy consumption, we offload users from high power macrocell to low power femtocells using our enhanced expected bitrate cell selection scheme. This scheme associates each mobile user to a base station which provides the maximum downlink bitrate considering the user load at base stations.

Second, efficient reuse of macrocell spectrum is proposed for femtocell downlink to maximize the overall system throughput. This, however, incurs additional interference to co-channel macrocell users. To handle this increased interference, we suggest Hybrid Constraint based Power Control (HCPC) technique. Since received signal and interference severely affect the channel quality of mobile users, we based our technique on a hybrid constraint which protects macro users based on the amount of interference it receives. Here, we divide macrocell users into two partitions; the ones those are protected by interference constraint and the rest by rate-loss constraint. To satisfy these constraints, power control over these reused macrocell subchannels is done while maximizing femto users' throughput.

The rest of the paper is organized as follows. Section 2 presents the system model for two-tier HetNet along with user partitioning, spectrum allocation technique, energy consumption analysis, and channel model. Section 3 discusses the hybrid constraint applicable on macrocell users. We formulate our problem in Section 4 along with the interference and rate-loss constraints. Performance analysis of different cell selection schemes for heterogeneous cellular network is done in Section 5. Section 6 discusses the optimization problem formulation and the relationship between interference and rate-loss constraint. Additionally, to improve femtocell throughput, we propose a technique to effectively reuse macrocell subchannels for femtocell users. Section 7 presents the simulation scenario and obtained results. The work is concluded in Section 8, with directions for future research.

## 2. System model

Our network model considers an overlay deployment of  $M$  Macro Base Stations (MBSs) and  $N$  FAPs, represented by sets  $\mathcal{M}$  and  $\mathcal{N}$ , respectively. The coverage region of each MBS (represented by  $H$ ) is assumed to be hexagonal. User Equipments (UEs) and FAPs are distributed in  $H$  as Homogeneous Spatial Poisson Point Process (SPPP) [21]. All FAPs are assumed to be in "Open Access" and hence can serve any UE within their range.

### 2.1. UE partitions

Overlay deployment of FAPs comes with the cost of increased co-tier and cross-tier interference to UEs. The value of signal strength and interference for the UEs in a network system depend on the distances from their serving and interfering base stations (BSs), and hence it is not uniform for all UEs. Additionally, due to different QoS requirements, some UEs can tolerate somewhat higher values of interference, without experiencing significant degradation in received bitrates.

Let  $\mathcal{U}$  represent the set of all UEs in the system. We divide these UEs into four different partitions based on their channel quality (Fig. 1). Femtocell UEs ( $\mathcal{U}_f$ ) are partitioned into *inner* and *outer* Femto UEs (FUEs). *Inner* FUEs,  $\mathcal{U}_f^I$ , are the UEs who receive high signal strength from their serving FAPs and/or low interference from neighbouring BSs. *Outer* FUEs,  $\mathcal{U}_f^O$ , are the ones which receive low signal strength from their serving FAPs due to high distance-dependent path loss and/or high interference from neighbouring BSs. Note that, FUEs are partitioned into *inner* and *outer*

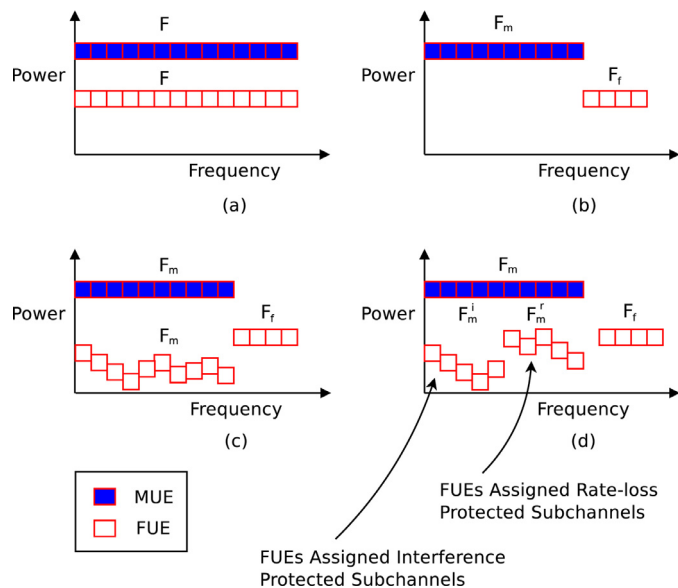
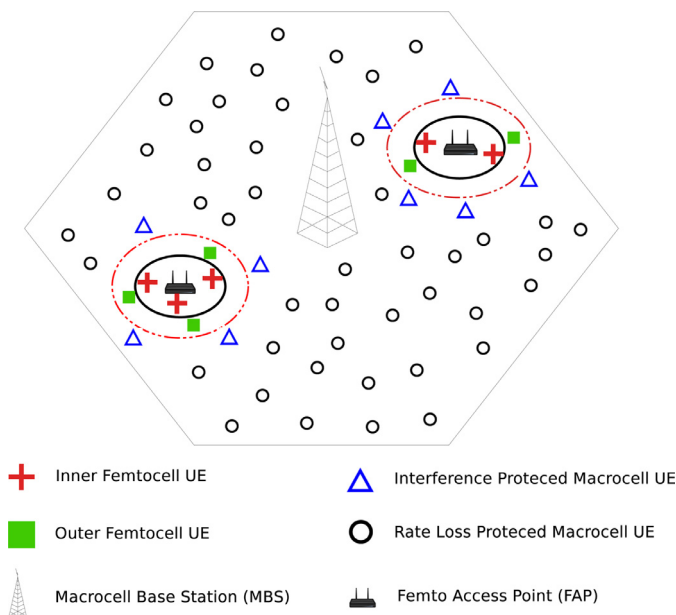


Fig. 2. Spectrum allocation between macrocell and femtocell.

FUEs based on the channel quality rather than their geographical location. Hence, *Outer* FUEs can include both femtocell edge UEs and the UEs offloaded to FAPs after applying cell biasing or some other offloading scheme.

In a similar manner, macro UEs ( $\mathcal{U}_m$ ) are divided into two partitions depending on the way they are protected from the FAP interference. First, the *interference protected* macrocell UEs,  $\mathcal{U}_m^i$ , are the ones which are very close to FAPs and hence receive high cross-tier interference. Second, the remaining *rate-loss protected* UEs ( $\mathcal{U}_m^r$ ), are those UEs which can tolerate rate loss, given the received interference at them is quite limited. Here,  $\mathcal{U}_f^i$ ,  $\mathcal{U}_f^o$ ,  $\mathcal{U}_m^i$ , and  $\mathcal{U}_m^r$  are mutually exclusive subsets. In Section 3, we discuss interference and rate-loss constraints in detail along with developing the relationship between them.

### 2.2. Spectrum allocation

The total available spectrum is assumed to be divided into  $F$  orthogonal frequency subchannels, each with a bandwidth of  $W$  Hz. Unless explicitly stated otherwise, it is assumed that all subchannels within a tier are assigned equal transmit power;  $P_{tx, m}$  for each MBS subchannel and  $P_{tx, f}$  for each FAP subchannel. In order to evaluate the performance of our approach, we consider the following three spectrum and power allocation techniques available in the literature.

- Reuse 1: Both MBS and FAPs use all available downlink subchannels for their UEs without any interference coordination technique. So, all  $F$  subchannels are allocated to MBS as well as to each FAP. This gives rise to high co-tier and cross-tier interference (Fig. 2(a)).
- Reuse  $\alpha$ : FAPs operate in spectrum orthogonal to the spectrum used by MBS. In this case, available  $F$  subchannels are partitioned as  $F_m = (1 - \alpha)F$  subchannels for MBS and  $F_f = \alpha F$  subchannels for each FAP. Such an allocation mitigates cross-tier interference, but there still exists co-tier or intra-tier interference among FAPs (Fig. 2(b)).
- Optimal Subchannel Power Allocation (OSPA): Power control based subchannel reuse techniques have proved to be an efficient way to improve system throughput [22]. The same had

been analysed in [23] where reuse of  $F_m$  macrocell subchannels is done for  $K$  strongest femto UEs with power control (Fig. 2(c)). The reuse is done in such a way that interference at macrocell users does not exceed some predefined threshold. This spectrum reuse for FAPs helps improving their throughput and reduce MBS energy consumption by UE offloading.

In this paper, we propose a power control technique in order to protect the channel quality of macrocell UEs based on the amount of interference experienced by them. Macrocell UEs are divided into two different groups and are protected by two different constraints namely interference and rate-loss constraints. Additionally, reuse of  $F_m$  macrocell subchannels is done for FUEs thereby improving system throughput. We divide  $F_m$  reuse subchannels into two sub-partitions,  $F_m^i$  and  $F_m^r$  (Fig. 2(d)). Subchannels in the set  $F_m^i$  are the ones assigned to MUEs which are protected by interference constraint. While,  $F_m^r$  set consists of the subchannels assigned to MUEs protected by rate-loss constraint. Here,  $F_m^i \cup F_m^r = F_m$  and  $F_m^i \cap F_m^r = \phi$ . Based on the underlying UE characteristics as described later, respective power control policy is applied over each sub-partition. We name it as Hybrid Constraint based Power Control (HCPC).

### 2.3. Energy consumption

Two different types of BSs are considered in our deployment scenario viz. MBS and FAP. Both of them differ significantly in terms of offered load and energy consumption. An MBS supports a much larger number of users over longer distance which is in contrast to a femtocell. Energy consumption of MBS is usually taken to be load dependent with some fixed “Zero Load” consumption. For FAPs, transmit power and number of users served are quite low, hence their energy consumption can be assumed to be independent of offered load and taken to be constant [24].

The total energy consumption of MBS can be calculated using the following equation [25],

$$E_{MBS} = E_0 + S \left( \frac{T_m}{\zeta_{PA}} + P_{SP} \right) (1 + C_{loss}) (1 + BP_{loss}) \quad (1)$$

where  $E_0$  is fixed “Zero Load” energy consumption.  $S$  and  $\zeta_{PA}$  represent the number of sectors and power amplifier efficiency, respectively.  $P_{SP}$  and  $C_{loss}$  represent the overhead for signal processing and cooling loss, respectively.  $BP_{loss}$  represents the

battery backup and power supply loss. Here  $T_m$  is total input power to transmitting antenna obtained by summing up transmit power ( $P_{tx,m}$ ) of all the subchannels in use.

For evaluation, we consider Energy Consumption Rating (ECR) as energy efficiency performance metric which is energy consumption normalized to throughput (Watts/Mbps) [26].

$$ECR = \frac{\text{Energy Consumption}}{\text{Effective System Throughput}} \quad (2)$$

Hence, the lower the value of ECR, the more energy efficient the system is.

#### 2.4. Channel model and variable bit-rate transmission

Considering OFDMA and round robin scheduling of subchannels for UEs, all subchannels within a tier can be considered to have identical characteristics over long term [27]. Rayleigh flat fading subchannels are considered to render them identically over long run. For co-channel femtocell deployment (Reuse 1), the instantaneous downlink (DL) SINR of UE when connected to MBS  $m$  at subchannel  $j$  is given by,

$$\Gamma_{j,m} = \frac{P_{tx,m}G_j^m}{1 + \sum_{l \in \mathcal{N}} P_{tx,l}H_j^l + \sum_{k \in \mathcal{M}, k \neq m} P_{tx,k}H_j^k} \quad (3)$$

Similarly, the instantaneous DL SINR of UE when connected to FAP  $k$ , at subchannel  $j$  is given by,

$$\Gamma_{j,F(k)} = \frac{P_{tx,f}G_j^k}{1 + \sum_{m \in \mathcal{M}} P_{tx,m}H_j^m + \sum_{l \in \mathcal{N}, l \neq k} P_{tx,l}H_j^l} \quad (4)$$

where  $G_j^k (H_j^k)$  is the effective signal (interference) gain to UE from base station  $k$  over subchannel  $j$ . For simplicity of the analysis, we normalize Gaussian noise power to 1. Hence, the term  $G_j^k (H_j^k)$  accounts for path loss and antenna gain normalised to Gaussian noise. When considering orthogonal subchannel assignment (Reuse  $\alpha$ ) between MBS and FAPs, the first summation term in the denominator of Eqs. (3) and (4) will disappear. Note that, we assume each subchannel within a base station is uniquely assigned to a single UE without sharing. Hence, we need not use any subscript in the SINR equations to identify the UE which is assigned a particular subchannel.

Based on DL SINR received at each UE, the instantaneous bitrate per subchannel is obtained by Shannon Hartley theorem [28] as,

$$B_{j,i} = W \log_2(1 + \Gamma_{j,i}) \quad \text{bits/s} \quad (5)$$

### 3. Hybrid constraint

In this section, we explain the hybrid constraint applicable on MUEs. In our work, MUEs are divided into two partitions based on their channel quality viz., *interference protected* MUEs and *rate-loss protected* MUEs. *Interference protected* MUEs are the ones who experience the worst channel quality due to low signal strength and/or high interference. For these MUEs, we use the *interference* constraint which protects their channel quality by controlling the interference over each subchannel assigned to them. On the other hand, *rate-loss protected* MUEs are the ones which can tolerate significant performance deterioration because they experience better signal strength from MBS and/or limited co-channel interference from FAPs. Such MUEs are protected by *rate-loss* constraint where we control the bitrate loss over each subchannel assigned to them. We now mathematically define both of these constraints in detail:

- **Interference constraint:** An MUE is said to be protected by interference constraint if for each subchannel  $j$  assigned to it, the total received interference from all FAPs does not exceed a certain threshold value. In order to do so, the transmit power of all

FAPs over each subchannel  $j$  is controlled using a power factor  $\Upsilon_j^k$ . Hence, interference constraint on MUE can be mathematically represented as,

$$\sum_{k \in \mathcal{N}} \Upsilon_j^k P_{tx,f} H_j^k \leq I_{max} \quad (6)$$

where  $\Upsilon_j^k$  is the power factor applied on subchannel  $j$  of FAP  $k$ . Here,  $I_{max}$  is the interference constraint applied to the subchannels to protect MUEs that are allocated subchannels belonging to the set  $F_m^i$ .

- **Rate-loss constraint:** This type of constraint defines an upper bound on the rate loss incurred by the macrocell users due to femtocell users' transmission over a shared subchannel. The rate loss experienced by a MUE over a subchannel depends upon the interference it receives from all the FAPs over that subchannel. By limiting the total interference over a subchannel, we can also limit the rate-loss for MUE over that subchannel. Let  $R_{j,m}^{lf}$  be the received bitrate at a MUE from MBS  $m$  at subchannel  $j$  in Reuse  $\alpha$  technique. This can be represented as,

$$R_{j,m}^{lf} = W \log_2(1 + P_{tx,m}G_j^m) \quad (7)$$

However, our suggested techniques (OSPA and HCPC) reuse  $F_m$  macrocell subchannels for FUEs with power control. This causes additional interference to MUEs and consequently lowers their received bitrate to  $R_{j,m}^{ll}$ ,

$$R_{j,m}^{ll} = W \log_2 \left( 1 + \frac{P_{tx,m}G_j^m}{1 + \sum_{l \in \mathcal{N}} \Upsilon_j^l P_{tx,f} H_j^l} \right) \quad (8)$$

here term  $\sum_{l \in \mathcal{N}} \Upsilon_j^l P_{tx,f} H_j^l$  represents the sum interference experienced by a MUE at subchannel  $j$  from all FAPs. Let  $\Delta R_j$  be the maximum rate loss an MUE can tolerate over subchannel  $j$ . Then, the following constraint should be satisfied,

$$R_{j,m}^{lf} - R_{j,m}^{ll} \leq \Delta R_j \quad (9)$$

Since  $R_{j,m}^{lf}$  and  $\Delta R_j$  are fixed for a simulation scenario, we define  $\tilde{R}_j = R_{j,m}^{lf} - \Delta R_j$ . Hence, after reuse of macrocell subchannels by FUEs, a MUE must receive a minimum bitrate  $R_{j,m}^{ll}$  over each subchannel  $j$  assigned to it as,

$$R_{j,m}^{ll} \geq \tilde{R}_j \quad (10)$$

### 4. Problem formulation & solution description

Our problem focuses on making the operation of cellular networks more energy efficient. We consider cell selection schemes such as RSRP (+ biasing) and expected bitrate based association to offload macrocell users to femtocells (lowering MBS energy consumption) and improving resource utilization for FAPs (improving system throughput). So, our main problem splits into two sub-problems:

- First, analysing the effect of different cell selection schemes on UE association, femtocell utilization and energy consumption. To compare RSRP and biasing based associations, we follow the approach of the authors in [29], with a few modifications to incorporate issues unique to femtocell. Then, we analyse expected bitrate based cell selection schemes which incorporate current load at base stations into cell selection criteria [13,14].
- Second, performing user association based on the optimal cell selection scheme obtained from above analysis, resulting in an increase in system throughput and reduction in energy consumption. Then, to further enhance the performance, we suggest efficient reuse of macrocell subchannels with power control for recently offloaded FUEs. Reuse is done in such a way

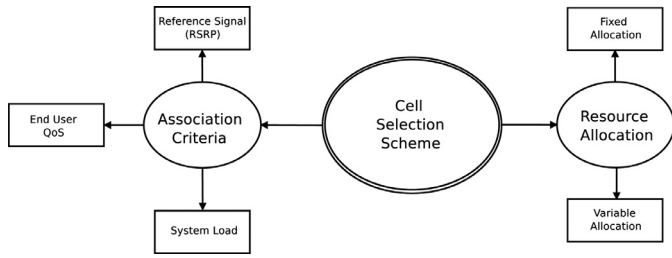


Fig. 3. Taxonomy for cell selection scheme.

that MUEs' channel quality is protected by two different constraints viz. interference constraint and rate-loss constraint. This results in further improvement in system throughput and energy efficiency.

## 5. Performance analysis of cell selection schemes

### 5.1. Cell selection schemes

In order to evaluate the performance of the network, we need to analyse the number of users in each tier and how this user association changes with different cell selection schemes. To systematically analyse the design aspects and performance of different cell selection schemes, we propose a taxonomy which consists of two non-overlapping branches – Association criteria and resource allocation technique as shown in Fig. 3. Association criteria defines the metric on which UEs get assigned to BSs. This metrics may include reference signal strength, UE QoS (such as downlink bitrate), and system load (such as user count and/or wireless resource utilization). Cell selection schemes can also be categories based on the underlying resource allocation technique. Two different categories of resource allocation techniques are considered for cell selection schemes. First is the fixed allocation where distribution of resources such as spectrum and transmit power among UEs remain fixed and is independent of the association criteria used. While, for variable resource allocation, the spectrum and transmit power allocation for UEs within a base station vary with time in order to improve the overall network performance. In this work, we focus our attention on the cell selection schemes which consider system load as association criteria and perform variable resource allocation to improve network throughput and energy efficiency. In this section, we analyse various cell selection schemes available in the literature.

#### 5.1.1. Max RSRP

This scheme considers Reference Signal Received Power (RSRP) based association for UEs. At the time of cell selection, UEs get associated with the BS providing highest RSRP [9]. So, the  $i$ th UE will select the  $j$ th BS as its serving BS if,

$$CellID_i = \arg \max_j (RSRP_j) \quad (11)$$

This scheme does not incorporate any information about the load at BS in the cell selection criteria. However, the simplicity of this scheme makes it practical for most real-world deployments [30,31]. As shown in Fig. 4, all UEs located within region 1 are associated with the FAP, while those located in regions 2 and 3 are associated with Macro Base Station (MBS).

#### 5.1.2. Max RSRP + Bias

Cell biasing modifies cell selection/handover criteria in order to improve user association in femtocells by actively pushing UEs in them [32]. With cell biasing, a Range Expansion Bias (REB) of  $\delta$  dB

is added to the RSRP value from FAPs before selection of serving BS. Then, the association of the UE  $i$  to the BS  $j$  is determined as,

$$CellID_i = \arg \max_j (RSRP_j + \delta_j) \quad (12)$$

where  $\delta_j$  is taken as 0 for MBS and some positive value for FAP  $j$ . This causes UEs to frequently select FAP as their serving BS. After biasing, UEs present in the shaded region of Fig. 4 will get offloaded to FAP. Additionally, these users are exposed to high interference from MBS. To protect their channel link quality, a fraction of bandwidth (say  $\alpha$ ,  $0 \leq \alpha \leq 1$ ) is reserved for these offloaded femtocell users thereby barring MBS to transmit on these sub-channels, while remaining bandwidth  $(1 - \alpha)$  is distributed among macro UEs.

#### 5.1.3. Max expected bitrate (E[B])

Authors in [13] have suggested that for improved throughput performance, bitrate received from the base station is a better criteria for cell selection than REB. Their proposed cell selection scheme assigns UEs to BSs which provide the highest expected bitrate,  $E[B]$ . Similar to Max RSRP + Bias scheme, Max  $E[B]$  allocates a fraction  $\alpha$  of total bandwidth to femto UEs, while the remaining bandwidth  $(1 - \alpha)$  is used by both macro and femto UEs. Then, expected bitrate for UE  $i$ , if connected to MBS is calculated as,

$$E[B_{i,m}] = (1 - \alpha)FW \log_2(1 + \Gamma_{i,m}^{IL}) \quad (13)$$

and if connected to FAP  $k$  is,

$$E[B_{i,k}] = (1 - \alpha)FW \log_2(1 + \Gamma_{i,k}^{IL}) + \alpha FW \log_2(1 + \Gamma_{i,k}^{IF}) \quad (14)$$

where  $\Gamma_{i,j}^{IL}$  and  $\Gamma_{i,j}^{IF}$  represent the SINR received at UE  $i$  from BS  $j$  on Interference Limited (IL) and Interference Free (IF) spectrum, respectively. Let  $\{BS\}$  represent the set of all base stations (MBSs + FAPs). UE  $i$  will select BS  $j$  as its serving BS if,

$$CellID_i = \arg \max_j \{E[B_{i,j}]; j \in \{BS\}\} \quad (15)$$

This cell selection scheme has been shown to improve performance of the system in terms of throughput and spectrum efficiency [13]. However, it considers the total available bandwidth at a BS rather than the bandwidth assignment to individual UEs and hence, leading to sub-optimal association of users.

#### 5.1.4. Enhanced expected bitrate (E[ $\hat{B}$ ])

We have proposed enhanced expected bitrate cell selection scheme for UEs ( $E[\hat{B}]$ ) which uses the bandwidth allotted per user, rather than total bandwidth at BS to make user association decisions [14].  $E[\hat{B}]$  not only takes care of current load and scheduling opportunities at a BS but also incorporates femtocell specific constraints on active connections and path loss. Using our proposed scheme, the expected bitrate obtained at UE  $i$  from MBS  $m$  is given by,

$$E[\hat{B}_{i,m}] = f(i, m, IL) (1 - \alpha)FW \log_2(1 + \Gamma_{i,m}^{IL}) \quad (16)$$

Similarly, the expected data rate at UE  $i$  from FAP  $k$  is,

$$E[\hat{B}_{i,k}] = f(i, k, IL) (1 - \alpha)FW \log_2(1 + \Gamma_{i,k}^{IL}) + f(i, k, IF) \alpha FW \log_2(1 + \Gamma_{i,k}^{IF}) \quad (17)$$

Here, function  $f(i, j, l)$  represents the fraction of subchannels available to UE  $i$  from BS  $j$  according to proportional fair allocation.  $f(i, j, l)$  makes sure that UEs get associated with BSs providing maximum achievable bitrate while keeping subchannel assignment count proportional to their SINRs. It also incorporates femtocell specific constraints so as to restrict UE association to infeasible FAPs. Here,

$$f(i, j, l) = \frac{1/\log_2(1 + \Gamma_{i,j}^l)}{\sum_{\forall k \in N_j} 1/\log_2(1 + \Gamma_{k,j}^l)} \times \mathbf{I}_{i,j,l} \quad (18)$$

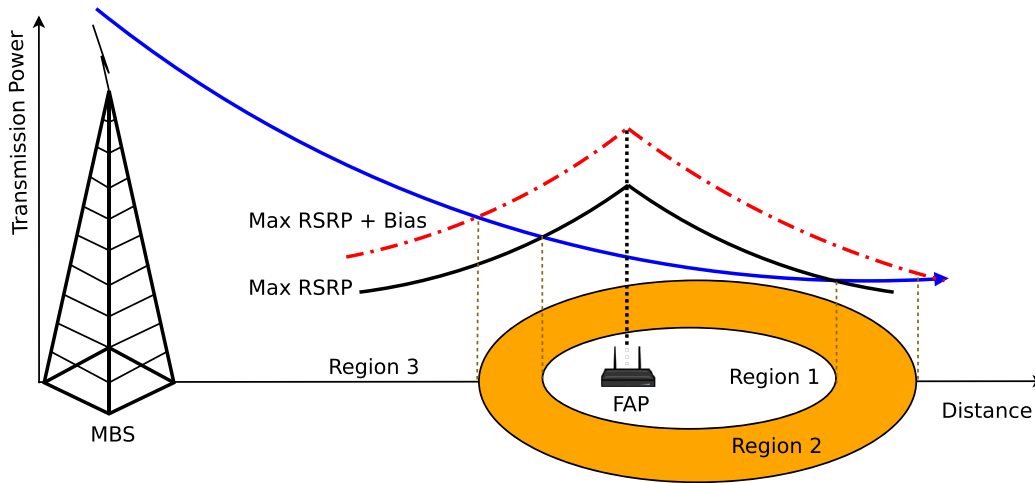


Fig. 4. User association with cell biasing.

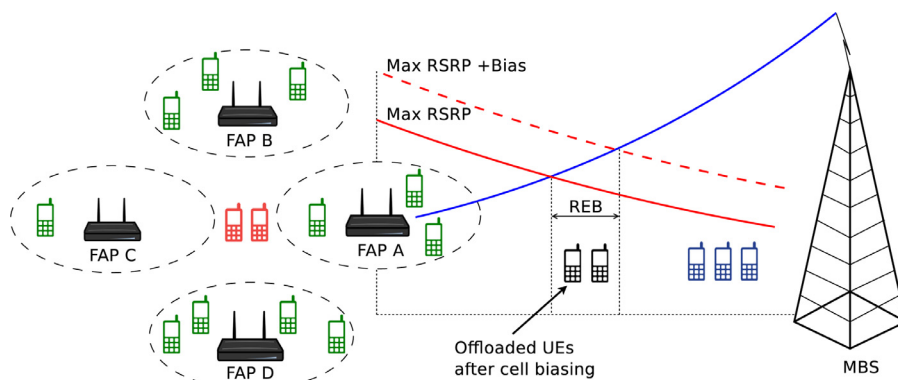


Fig. 5. Deployment scenario.

where  $\mathbf{I}_{i,j,l}$  is an indicator random variable that takes care of maximum number of users and minimum threshold SINR constraints. Hence,

$$\mathbf{I}_{i,j,l} = \begin{cases} 1, & \text{if } N_j < C_{max} \text{ and } \Gamma_{i,j}^l \geq \Gamma_{thresh} \\ 0, & \text{otherwise} \end{cases} \quad (19)$$

where  $N_j$  is the number of UEs currently served by FAP  $j$  and  $\Gamma_{thresh}$  is threshold for downlink SINR. Here,  $C_{max}$  represents the maximum number of simultaneous connections that can be supported by an FAP.

Therefore, according to enhanced expected bitrate scheme, UE  $i$  will select BS  $j$  as its serving BS if,

$$CellID_i = \max_j \{E[\hat{B}_{i,j}]; \forall j \in \{BS\}\} \quad (20)$$

### 5.2. Performance analysis

To study the performance of various cell selection schemes, consider a deployment scenario as shown in Fig. 5. RSRP based association schemes (Max RSRP and Max RSRP+Bias) use received signal strength as the key parameter to perform user association. RSRP at a UE is calculated as a linear average of signal power on cell-specific reference signals within the considered bandwidth. This typically excludes intra and cross-tier interference and noise. Hence, an association based on received signal strength may not be the best in terms of received signal quality. As can be seen in Fig. 5, green coloured UEs couple themselves with different FAPs as they receive higher RSRP from them. The remaining UEs (Black and blue UEs) receive higher RSRP from MBS and hence select

MBS as their target BS. This scheme typically fails to consider signal quality, bandwidth and load at target base station. Not only that, low transmission power capability of FAPs results in very low user count in them. The same can be observed in Fig. 6(a) where the number of FUE (FUE Count) is lowest among all cell selection schemes. Consequently, this results in low femtocell utilization and lesser femtocell throughput (Fig. 6(b)). Additionally, we can see that total MBS energy consumption is highest for Max RSRP case because macrocell still has to serve large number of UEs due to limited offloading (Fig. 6(c)). The simulation parameters for obtaining these results are given in Table 1.

Cell biasing facilitates UE offloading by adding an REB to RSRP from FAPs. Note that, this does not change the transmission power of femtocell. It only prioritizes the selection of FAPs by adding a positive value to received RSRP. See Fig. 5, where some UEs (Black UEs) get offloaded from MBS to FAPs after biasing. Consequently, this results in improvement of femtocell throughput and reduction of MBS energy consumption (Fig. 6). Further incrementing REB will offload a higher number of users to FAPs. However, increasing REB beyond a certain value is not recommended. It has been observed that REB value greater than 8 dB is infeasible in most practical deployments as it abruptly increases the UE count in femtocells and consequently competition for femtocell resources [29]. Cell biasing guarantees UE offloading but do not promise improvement in end users' bitrates.

Considering end users' perspective, the most important performance metric is received bitrate. Received bitrate at a UE is a function of SINR and allotted bandwidth. High transmit power from MBS causes more UEs association in them. This accords UEs with

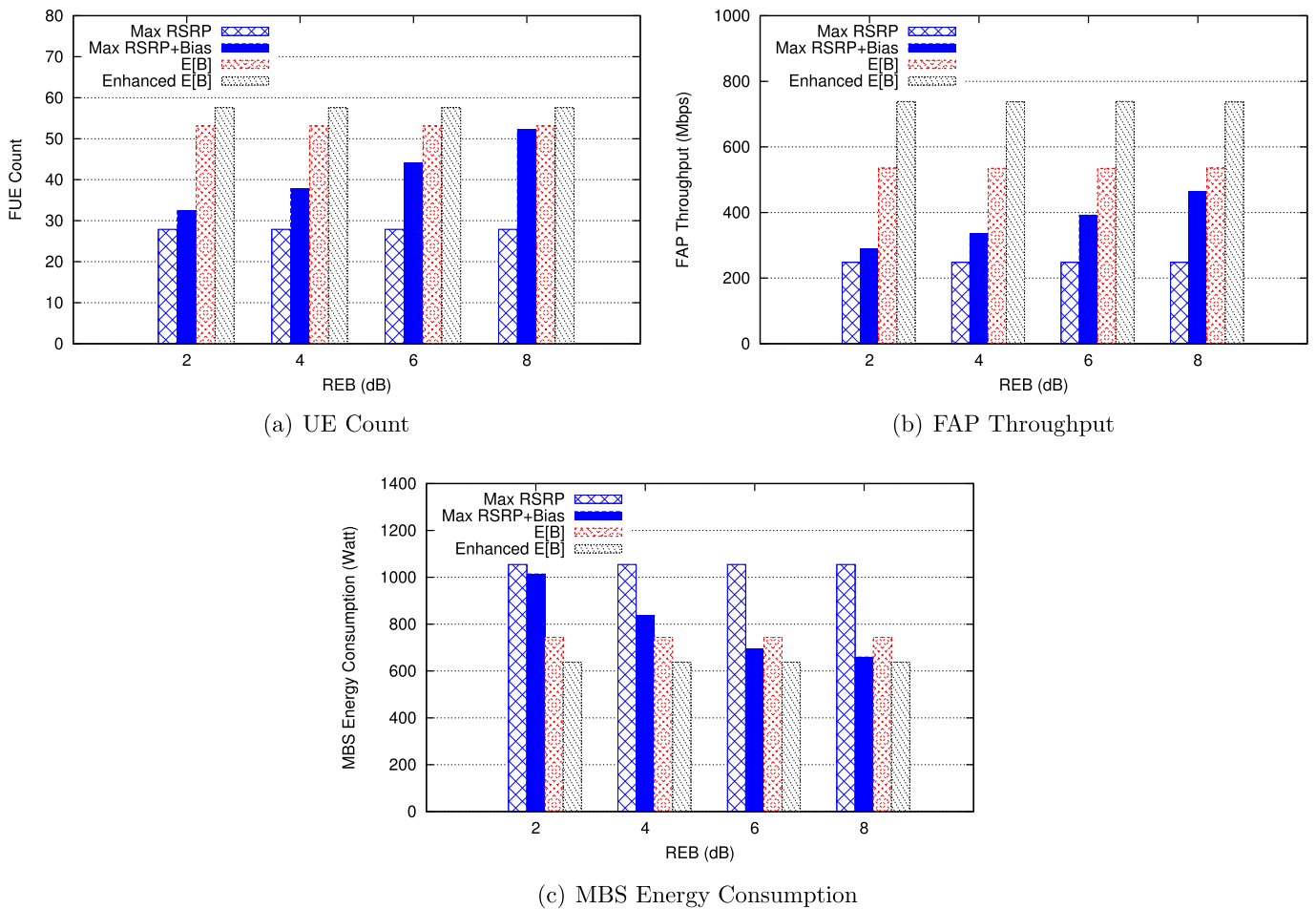


Fig. 6. Performance analysis of cell selection schemes for varying REB.

high SINR, but they receive lower bandwidth due to stiff competition of resources among associated UEs. On the contrary, FAPs can offer much higher bandwidth to associated UEs. However, their transmission power limitation also limits received SINR at UEs.

We now study expected bitrate based association schemes ( $E[B]$  and  $E[\hat{B}]$ ), which incorporate received bitrate in cell selection criteria rather than received signal strength.  $E[B]$  suggests to allocate a fraction of bandwidth exclusively to FUEs and then calculates expected bitrate from each BS in range. Finally, UE gets associated with a BS providing highest expected bitrate. Note that, this scheme calculates expected bitrate based on total available bandwidth rather than unallocated bandwidth at the target BS. Hence, UEs which are equidistant from many FAPs (for example, Red UEs in Fig. 5) can select any nearby FAP as target. Since fraction of bandwidth available at FAPs is much higher than MBS, we see quite a number of UEs offloaded to femtocell (Fig. 7). Consequently, we observe improvement in femtocell throughput and reduction in MBS energy consumption compared to Max RSRP and cell biasing (Fig. 7).

An improvement to  $E[B]$  scheme is to incorporate offered load into cell selection criteria. If a UE is equidistant from multiple FAPs, it will receive equal SINR from all of them. However, bandwidth allotted to it depends on the load at target BS. Enhanced expected bitrate scheme ( $E[\hat{B}]$ ) incorporates this fact by calculating expected bitrate from MBS and all FAPs considering residual bandwidth. This scheme allows UEs to distinguish among FAPs based on the number of associated UEs along with their bitrates. Hence, some UEs (Red coloured) now get associated with only FAP C (Fig. 5) because

it might provide the same SINR as other nearby FAPs but grants higher bandwidth because of low resource competition. Consequently, this results in highest user association, FAP throughput, and lowest MBS energy consumption among all schemes (Fig. 7). Furthermore, with increasing  $\alpha$ , more and more UEs get offloaded to FAPs, consequently improving UE count and FAP throughput. Note that, for varying  $\alpha$ , the FUE count remains unchanged for Max RSRP and Max RSRP + Bias. This results from the fact that these schemes make use of RSRP and REB to make association decision rather than the value of  $\alpha$ . Similar trends are observed for  $E[B]$  and  $E[\hat{B}]$  for varying REB (Fig. 6). The UE count, FAP throughput, and MBS energy consumption remain unchanged for varying REB. This is due to the fact that user association in  $E[B]$  and  $E[\hat{B}]$  is based on received bitrate rather than RSRP.

## 6. Optimization problem formulation

Once required number of users get offloaded to femtocells through biasing or expected bitrate based association, we focus on improving femtocell throughput. Let  $N_k$  be the number of UEs associated with femtocell  $k$  and total number of FUEs in the system can be denoted as  $|\mathcal{U}_f| = \sum_k N_k$ . Considering flat fading subchannels, the SINR received at a UE on each assigned subchannel will be the same. Let  $\theta_k$  be the number of inner FUEs in FAP  $k$ . The total throughput obtained for FAP  $k$  will be the sum total of three different throughput entities i.e. a) throughput obtained by the outer  $N_k - \theta_k$  FUEs, b) throughput obtained by the inner  $\theta_k$  FUEs, and c) throughput obtained by inner  $\theta_k$  FUEs by reusing the macrocell subchannels. Considering all subchannels assigned to an UE have

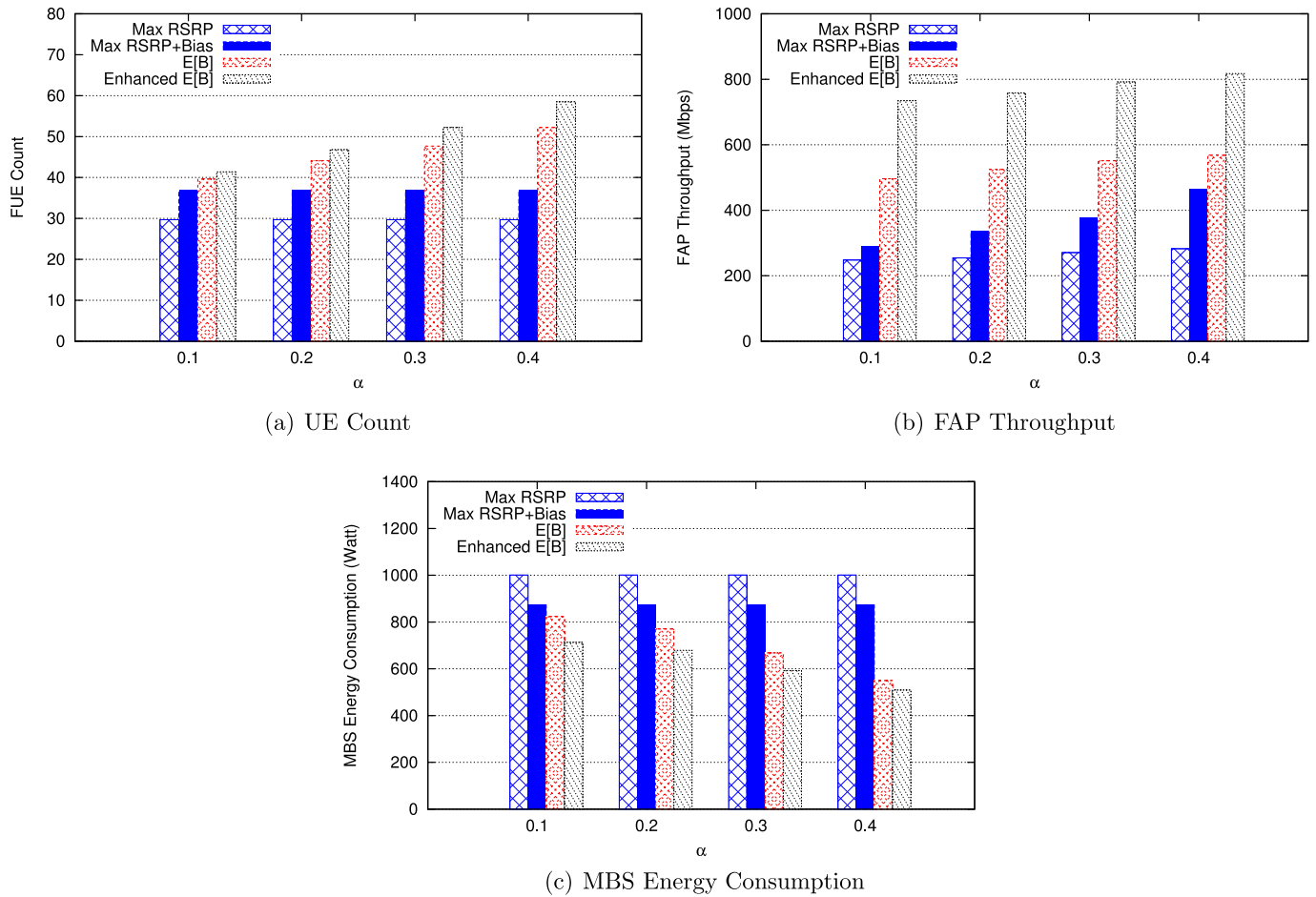


Fig. 7. Performance analysis of cell selection schemes for varying  $\alpha$ .

identical characteristics, the total throughput of FAP  $k$  can be represented mathematically as,

$$\chi_k = \sum_{i=\theta_k+1}^{N_k} \sum_{j \in \mathfrak{N}_i} W \log_2(1 + \Gamma_{j,F(k)}) + \sum_{i=1}^{\theta_k} \sum_{j \in \mathfrak{N}_i} W \log_2(1 + \Gamma_{j,F(k)}) + \xi_k \quad (21)$$

where array  $\mathfrak{N}_i$  represents the set of subchannels assigned to FUE  $i$ . For simplicity, we equally allocate subchannels among FUEs, hence,  $|\mathfrak{N}_i| = F_f/N_k$  for all  $i$ . Note that, our problem formulation is valid for disproportionate channel assignment schemes too. The last term,  $\xi_k$ , which represents the throughput gain obtained by reusing  $F_m$  subchannels with power control can be obtained as,

$$\xi_k = \sum_{j=1}^{F_m} W \log_2(1 + \Upsilon_j^k P_{tx,f} G_j^k) \quad (22)$$

where  $\Upsilon_j^k$  is the power factor applied for transmission on subchannel  $j$  of FAP  $k$ . Note that, here we assume no interference to femtocell users over  $F_m$  subchannels due to high wall penetration loss.

Our objective is to maximize the sum throughput of all femtocells over these  $F_m$  subchannels while satisfying interference and rate loss constraint which can be further translated into bitrate and maximum transmit power constraints. Thus, we formulate our optimization problem as,

$$\text{Maximize}_{\Upsilon_j^k} \sum_{k \in \mathcal{N}} \xi_k \quad (23)$$

Subject to,

$$\sum_{k \in \mathcal{N}} \Upsilon_j^k P_{tx,f} H_j^k \leq I_{max} \quad \forall j \in F_m^i \quad (24)$$

$$R_{j,m}^{LL} \geq \tilde{R}_j \quad \forall j \in F_m^r \quad (25)$$

$$\sum_{j \in F_m} \Upsilon_j^k * P_{tx,f} \leq F_m * P_{tx,f} \quad \forall k \quad (26)$$

$$\Upsilon_j^k \geq 0 \quad \forall j, k \quad (27)$$

$$F_m^i \cup F_m^r = F_m \quad (28)$$

where  $[Y]_{j \times k}$  is the matrix containing power factor values for each subchannel of each FAP. Eqs. (24) and (25) represent interference and bitrate constraints applicable on macrocell users. Eq. (26) is the maximum transmit power constraint for FAPs over these  $F_m$  subchannels. When optimization is performed over these  $F_m$  subchannels, the transmit power of few subchannels is reduced (where  $\Upsilon_j^k < 1$ ) and the residual power can be redistributed among the rest of the subchannels while keeping sum transmit power constant.

To solve this problem, we propose a centralized algorithm which determines the power factor values for each subchannel of each FAP. We assume that the centralized algorithm has instantaneous information about all the gains (signal and interference)



**Table 1**  
Simulation parameters.

Parameter	Value
Bandwidth	10 MHz
Simulation area	12.35 km <sup>2</sup>
No. of subchannels	256
MBS radius	500 m
FAP radius	15 m
MBS transmit power	43 dBm
FAP transmit power	23 dBm
Wall loss	10 dB
UE density	100/km <sup>2</sup>
FAP density	{5 – 20}/km <sup>2</sup>
Reuse factor ( $\alpha$ )	{0.1 – 0.4}
Gaussian noise figure	–174 dBm/Hz
FAP energy consumption	10 W
Zero-load MBS energy ( $E_0$ )	500 W
Number of sectors ( $S$ )	1
$S_{PA}$	0.15
$P_{SP}$	200 W
$C_{loss}$	0.35
$BP_{loss}$	0.25
Range expansion bias (REB)	{0, 2, 4, 6, 8}
Path loss coefficient	MBS 2.5 FAP 3.5
Antenna gain	MBS 14 dB FAP 7 dB UE 0 dB

either through FAP backhaul or by uplink signal estimation. To solve the above problem, we make use of Lagrange's dual method [33,34]. By solving the dual problem instead of the primal one allows us to obtain the lower bound on the optimal solution. This is done by incorporating the constraints directly into the original objective function. In practice, the dual problem can often be solved more easily than the original optimization problem. Hence, we formulate the Lagrangian of the problem as,

$$\begin{aligned} \mathcal{L}(\Upsilon_j^k, \{\mu_j\}, \{\lambda_k\}, \{\phi_j\}) = & \sum_{k \in \mathcal{N}} \sum_{j \in F_m} W \log_2(1 + \Upsilon_j^k P_{tx,f} G_j^k) \\ & - \sum_{j \in F_m} \mu_j \left( \sum_{k \in \mathcal{N}} \Upsilon_j^k P_{tx,f} H_j^k - I_{max} \right) \\ & - \sum_{j \in F_m} \phi_j (\tilde{R}_j - R_{j,m}^L) \\ & - \sum_{k \in \mathcal{N}} \lambda_k \left( \sum_{j \in F_m} \Upsilon_j^k - F_m \right) \end{aligned} \quad (29)$$

where  $\mu_j$ ,  $\phi_j$  and  $\lambda_k$  are non-negative Lagrange multipliers for interference, bitrate and transmit power constraints, respectively. Note that constraints in the above optimization problem are non-convex. Therefore, solving this problem by converting it into Lagrange dual problem may result in non-zero duality gap between the primal problem and its dual problem. However, *time-sharing* condition applicable for realistic (large) number of subchannels allows us to solve the problem using Lagrange's dual method with close to zero duality gap, hence providing near optimal solution [27,33].

Using dual decomposition method [33,35], the above problem can be split up into two sub-problems – **Problem: A** and **Problem: B** with respective Lagrangian represented as,

#### Problem: A

$$\begin{aligned} \mathcal{L}'(\Upsilon_j^k, \{\mu_j\}, \{\lambda_k\}) = & \sum_{k \in \mathcal{N}} \sum_{j \in F_m} W \log_2(1 + \Upsilon_j^k P_{tx,f} G_j^k) \\ & - \sum_{j \in F_m} \mu_j \left( \sum_{k \in \mathcal{N}} \Upsilon_j^k P_{tx,f} H_j^k - I_{max} \right) - \sum_{k \in \mathcal{N}} \lambda_k \left( \sum_{j \in F_m} \Upsilon_j^k - F_m \right) \end{aligned} \quad (30)$$

#### Problem: B

$$\begin{aligned} \mathcal{L}''(\Upsilon_j^k, \{\lambda_k\}, \{\phi_j\}) = & \sum_{k \in \mathcal{N}} \sum_{j \in F_m} W \log_2(1 + \Upsilon_j^k P_{tx,f} G_j^k) \\ & - \sum_{j \in F_m} \phi_j (\tilde{R}_j - R_{j,m}^L) - \sum_{k \in \mathcal{N}} \lambda_k \left( \sum_{j \in F_m} \Upsilon_j^k - F_m \right) \end{aligned} \quad (31)$$

To solve Problem A, we divide it into  $F_m$  independent sub-problems, one for each subchannel, while keeping  $\lambda_k$  fixed. Hence, the sub-problem for any subchannel  $j \in F_m$  is represented as,

$$\begin{aligned} \max_{\Upsilon_j^k} \sum_{k \in \mathcal{N}} W \log_2(1 + \Upsilon_j^k P_{tx,f} G_j^k) \\ - \mu_j \left( \sum_{k \in \mathcal{N}} \Upsilon_j^k P_{tx,f} H_j^k - I_{max} \right) \\ - \sum_{k \in \mathcal{N}} \lambda_k (\Upsilon_j^k - F_m) \end{aligned} \quad (32)$$

In order to maximize the above Lagrangian, derivative of Eq. (32) with respect to  $\Upsilon_j^k$  is taken. Considering the non-negative power constraint in Eq. (27), we have,

$$\Upsilon_j^k = \max(0, Q(\mu_j)) \quad (33)$$

where

$$Q(\mu_j) \equiv \left( \frac{W}{\mu_j P_{tx,f} H_j^k + \lambda_k} - \frac{1}{P_{tx,f} G_j^k} \right) \quad (34)$$

Substituting  $\Upsilon_j^k$  in Eq. (24) gives us,

$$\sum_{k \in \mathcal{N}} \max(0, Q(\mu_j)) P_{tx,f} H_j^k \leq I_{max} \quad (35)$$

For fixed  $\lambda_k$ , we can see that  $Q(\mu_j)$  is a decreasing function of  $\mu_j$  which obtains maximum value when  $\mu_j = 0$ . If LHS in Eq. (35) is smaller than RHS, we can set  $\mu_j$  equals to zero. If not, the value of  $\mu_j$  can be easily calculated by solving Eq. 35 with equality.

#### 6.0.1. Relationship between interference constraint & rate-loss constraint

To solve Problem B, we first investigate the relationship between interference and rate-loss constraints. This will help us to prove that interference power constraint can serve as an upper bound on rate-loss of MUE. Additionally, this will simplify Problem B by representing its non-convex rate-loss constraint as an equivalent interference constraint.

We claim that there exists an interference threshold,  $\overline{I_{max}^j}$ , for subchannel  $j$  such that the rate-loss incurred on that subchannel is less than  $\Delta R_j$ . Using Eq. (8), received bitrate at an MUE is represented as,

$$\begin{aligned}
 R_{j,m}^{ll} &= W \log_2 \left( 1 + \frac{P_{tx,m} G_j^m}{1 + \sum_{l \in \mathcal{N}} \Upsilon_j^l P_{tx,f} H_j^l} \right) \\
 &\geq W \log_2 (1 + P_{tx,m} G_j^m) - W \log_2 \left( 1 + \sum_{l \in \mathcal{N}} \Upsilon_j^l P_{tx,f} H_j^l \right) \\
 &\geq R_{j,m}^{lf} - W \log_2 \left( 1 + \sum_{l \in \mathcal{N}} \Upsilon_j^l P_{tx,f} H_j^l \right) \quad (36)
 \end{aligned}$$

Replacing  $R_{j,m}^{lf} - R_{j,m}^{ll}$  by  $\Delta R_j$  and considering  $\overline{I_{max}^j} \geq \sum_{l \in \mathcal{N}} \Upsilon_j^l P_{tx,f} H_j^l$ , we can make sure that maximum rate loss is upper bounded by  $\log_2(1 + \overline{I_{max}^j})$ . Hence,

$$\Delta R_j \leq W \log_2 \left( 1 + \sum_{l \in \mathcal{N}} \Upsilon_j^l P_{tx,f} H_j^l \right) \leq W \log_2 (1 + \overline{I_{max}^j}) \quad (37)$$

We can regulate the rate-loss to be less than  $\Delta R_j$  by choosing this interference threshold for subchannel  $j$  as,

$$\overline{I_{max}^j} \geq \sum_{l \in \mathcal{N}} \Upsilon_j^l P_{tx,f} H_j^l \geq 2^{\Delta R_j/W} - 1 \quad (38)$$

Hence Lagrangian of **Problem B** can be re-written as,

$$\begin{aligned}
 \mathcal{L}''(\Upsilon_j^k, \{\lambda_k\}, \{\phi_j\}) &= \sum_{k \in \mathcal{N}} \sum_{j \in F_m} W \log_2 (1 + \Upsilon_j^k P_{tx,f} G_j^k) \\
 &\quad - \sum_{j \in F_m} \phi_j \left( \sum_{l \in \mathcal{N}} \Upsilon_j^l P_{tx,f} H_j^l - (2^{\Delta R_j/W} - 1) \right) \\
 &\quad - \sum_{k \in \mathcal{N}} \lambda_k \left( \sum_{j \in F_m} \Upsilon_j^k - F_m \right) \quad (39)
 \end{aligned}$$

To solve this problem, we divide it into  $F_m$  independent sub-problems, similar to Problem A. Keeping  $\lambda_k$  fixed, we then take derivative of Lagrangian with respect to  $\Upsilon_j^k$ . Then, using a method similar to the one given in [27], it can be shown that the optimal power allocation is,

$$\Upsilon_j^k = \max(0, P(\phi_j)) \quad (40)$$

where

$$P(\phi_j) \equiv \left( \frac{W}{\phi_j P_{tx,f} H_j^k + \lambda_k} - \frac{1}{P_{tx,f} G_j^k} \right) \quad (41)$$

The non-negative dual variable  $\phi_j$  (associated with the rate-loss constraint) either equals zero or is determined by solving the following equation with equality,

$$\sum_{l \in \mathcal{N}} \max(0, P(\phi_j)) P_{tx,f} H_j^l \leq (2^{\Delta R_j/W} - 1) \quad (42)$$

**Algorithm 1** represents the sequence of steps to solve the original optimization problem. It iteratively calculates  $\mu_j$  and  $\phi_j$  until the desired accuracy is achieved, while updating  $\lambda_k$  using sub-gradient algorithm. Once all  $\mu_j$ 's and  $\phi_j$ 's are determined, power factor values are calculated. Using Eqs. (33) and (40), the centralized algorithm constructs a matrix  $[Y]_{j \times k}$  containing power factor values for each FAP's subchannel. Finally, these values are communicated to FAPs in order to perform appropriate power control so as to mitigate interference to MUEs.

We propose the use of a centralised algorithm for power factor calculation instead of a distributed one because of the dynamic network characteristics of femtocell networks such as FAP locations and their ON – OFF status. However, **Algorithm 1** can also be implemented in a distributed fashion. For this, we can run **Algorithm 1** for each UE in a distributed manner to calculate the

**Algorithm 1** Power factor calculation.

```

Initialize  $\lambda_1, t = 1$ 
repeat
  for each subchannel  $j \in \{F_m^i \cup F_m^r\}$  do
    Compute
     $S = \sum_{k \in \mathcal{N}} \max\left(0, \frac{W}{\lambda_k} - \frac{1}{P_{tx,f} G_j^k}\right) P_{tx,f} H_j^k$ 
    if  $j \in F_m^i$  and  $S < I_{max}$  then
      Set  $\mu_j = 0$ 
    else
      Find  $\mu_j$  that satisfies Eq. (35) with equality.
      Calculate  $\Upsilon_n^m, \forall n \in F_m^i$  using Eq. (33).
    end if
    if  $j \in F_m^r$  and  $S < 2^{\Delta R_j/W} - 1$  then
      Set  $\phi_j = 0$ 
    else
      Find  $\phi_j$  that satisfies Eq. (42) with equality.
    end if
    Calculate  $\Upsilon_n^m, \forall n \in F_m^r$  using Eq. (40).
  end for
  Update  $\lambda_{t+1} = \lambda_t - \nu \left( F_m - \sum_{i=1}^m \Upsilon_i^k \right)$ 
  if  $\lambda_{t+1} < 0$  then
    Set  $\lambda_{t+1} = 0$  and stop
  end if
until  $(\lambda_{k+1} - \lambda_k)^2 \leq \varepsilon$  Note : Here,  $\lambda_t$  is a column vector of size  $k$  at iteration  $t$ ,  $\nu$  is the step size, and  $\varepsilon$  is a positive small number to define convergence.
    
```

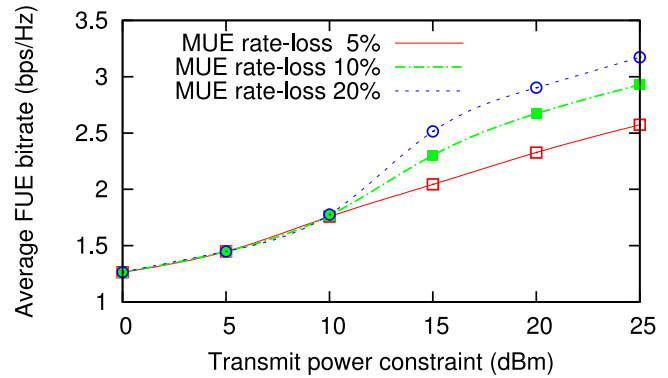


Fig. 8. Average FUE spectral efficiency.

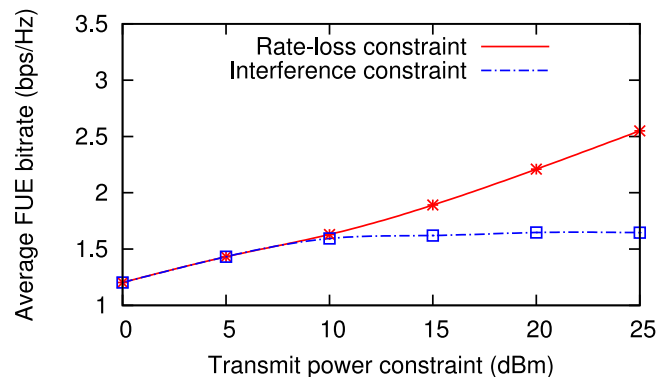


Fig. 9. Comparing interference vs. rate-loss constraint.

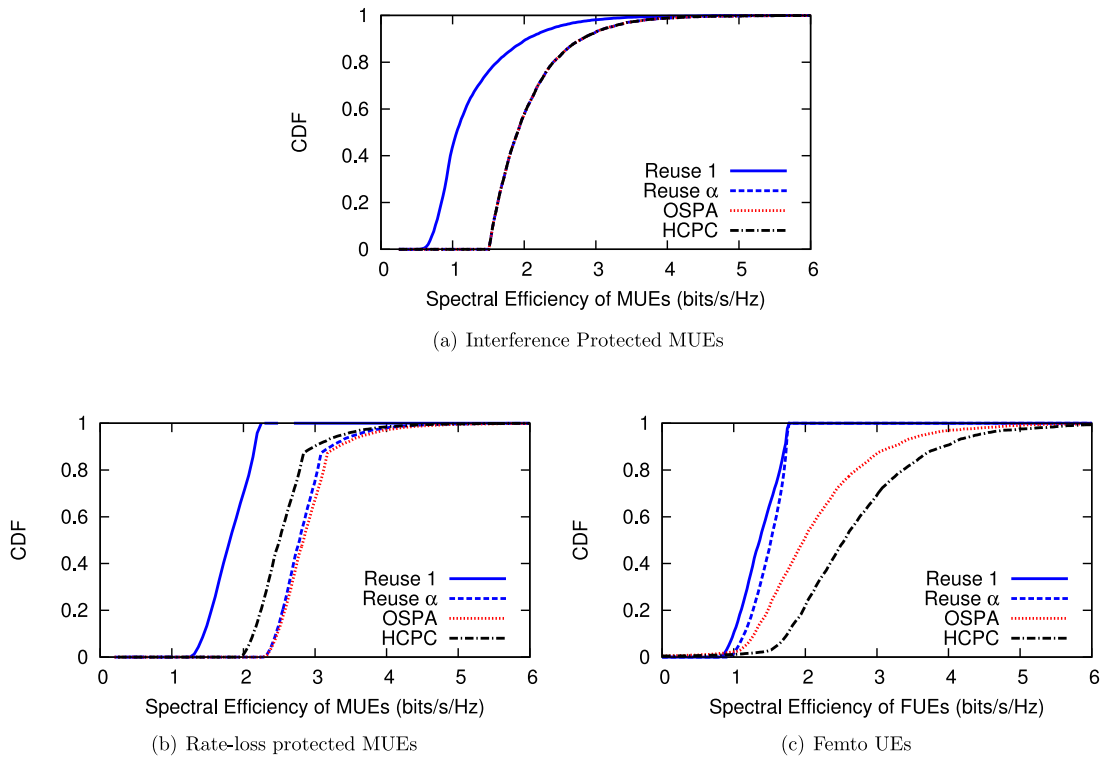
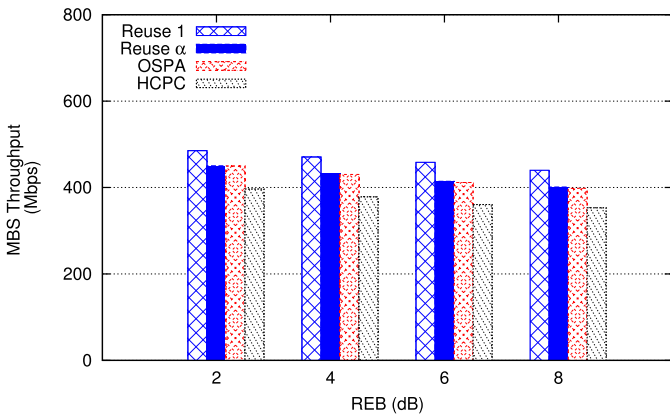
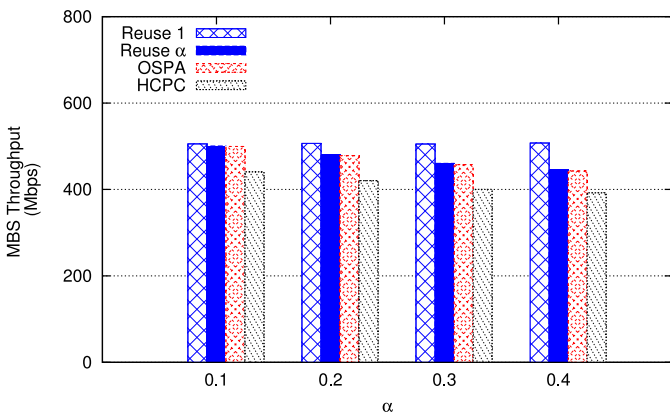


Fig. 10. CDF of UEs' spectral efficiency.



(a) MBS Throughput vs. REB for Max RSRP+Bias



(b) MBS Throughput vs.  $\alpha$  for  $E[\hat{B}]$

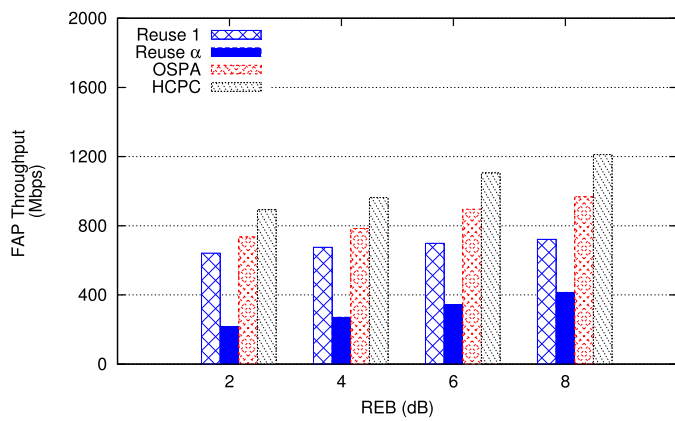
Fig. 11. MBS throughput.

subchannel power factor values of its interfering FAPs. Either the UE or one of the interfering FAPs can be chosen as a central entity to perform the local optimization. Though this approach is computationally less intensive, it may not result in calculating the globally optimal power factor values for all FAPs. The design of such a distributed algorithm is beyond the scope of this paper and hence left for future work.

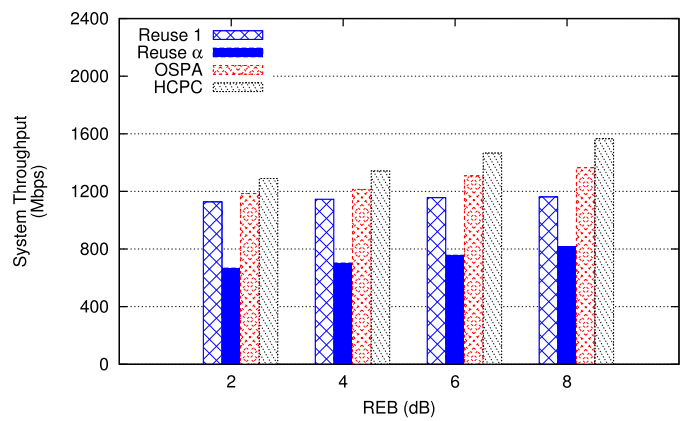
7. Simulation results

Our simulation scenario assumes an LTE-A compliant 19-cell hexagonal wrap-around cellular model overlaid with low power FAPs [36]. Both UEs and FAPs are distributed using homogeneous SPPP in the covered region. We run the simulation considering full buffer traffic model i.e., UEs always have some data to send. Femtocells are assumed to be in *Always-ON* state unless there are no UEs under its coverage. Snapshots are taken at discrete time intervals. Based on statistics of subchannels used by UEs, values of power factor are calculated. The interference threshold,  $I_{max}$ , is taken to be 1% of femtocell subchannel transmit power ( $0.01 * P_{tx,f}$ ). Simulation results are averaged over 60 deployment scenarios and are plotted with 95% confidence interval. The rest of the simulation parameters are given in Table 1.

We first analyse the effect of interference and rate-loss constraints on bitrate and spectral efficiency of MUEs and FUEs. Fig. 8 shows the effect of rate-loss constraint on average spectral efficiency of FUEs. As we can see that spectral efficiency of FUEs keeps improving with increase in maximum transmit power constraint (Eq. (26)). Assume that the values of rate-loss that can be tolerated by an MUE lie in the set  $S = \{5\%, 10\%, 20\%\}$ . Then, for satisfying per subchannel rate-loss constraint, the interference threshold  $I_{max}^j$  is taken as  $2^{\Delta R_j/W} - 1$ , where  $\Delta R_j = \{s * R_{s,m}^{LF}/100\}$ ,  $\forall s \in S$ . It is observed that as percentage of tolerable rate loss increases for MUEs, spectral efficiency of FUEs also increases. This is due to the fact that when higher rate-loss is acceptable, FAPs can transmit at higher power to their UEs without significantly affecting the re-



(a) FAP Throughput vs. REB for Max RSRP+Bias



(a) System throughput vs. REB for Max RSRP+Bias

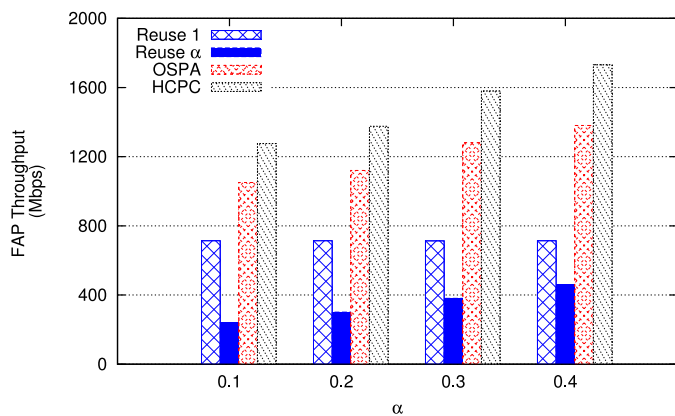
(b) FAP Throughput vs.  $\alpha$  for  $E[\hat{B}]$ 

Fig. 12. FAP throughput.

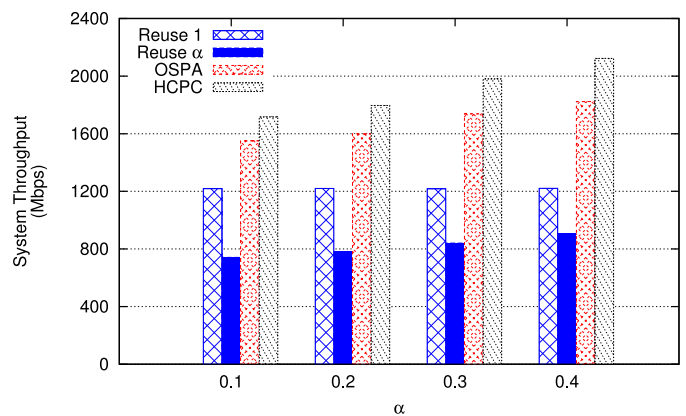
(b) System throughput vs.  $\alpha$  for  $E[\hat{B}]$ 

Fig. 13. System throughput.

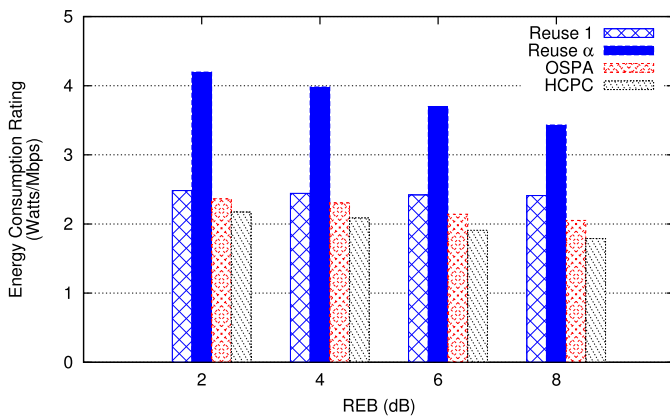
ceived bitrate of MUEs. It is also observed that when maximum transmit power constraint over  $F_m$  is small, the spectral efficiency of FUEs for different percentage of rate-loss is almost the same. This results from the fact that, for lower value of  $F_m * P_{tx, f}$ , transmit power constraint is more dominant than rate-loss constraint. As maximum transmit power over  $F_m$  increases, rate-loss constraint becomes the dominant constraint, thereby showing considerable difference in spectral efficiency of FUEs.

Fig. 9 shows comparison of per subchannel rate-loss constraint and per subchannel interference constraint. As we can see that average spectral efficiency of FUEs under rate-loss constraint is nearly the same as interference constraint for lower values of maximum transmit power ( $F_m * P_{tx, f}$ ). However, as this transmit power increases, we observe quite an improvement in spectral efficiency of FUE for rate-loss constraint compared to interference constraint. This improvement in FUEs' spectral efficiency is direct consequence of allowing FAPs to transmit at higher power while satisfying MUEs' rate-loss constraint.

To analyse the performance of all four spectrum allocation techniques, a random allocation of  $F_m$  subchannels among MUEs is done, while satisfying minimum bitrate constraint. Additionally, for OSPA and HCPC, we adapt subchannel transmit power in order to maximize spectral efficiency of femtocell UEs (Measured in bits/s/Hz). OSPA and HCPC are independent of the subchannel allocation policy used after spectrum partitioning between MBS and FAPs, and can work with any allocation policy such as equal, proportionate, and fair allocation. OSPA and HCPC improve femtocell throughput irrespective of the underlying policy in use.

Fig. 10 depicts the Cumulative Distribution Function (CDF) of spectral efficiency of macro and femto UEs for all spectrum allocation techniques. As we can see, CDF of MUEs improves for Reuse  $\alpha$  compared to Reuse 1 (Fig. 10(a) and 10(b)). This results from the reduced co-channels interference from femtocell to MUEs due to orthogonal spectrum reuse. A similar improvement is observed for OSPA and HCPC as these techniques also eliminate interference to MUEs via frequency partitioning. A key observation is that, for interference protected MUE, the curves of OSPA, HCPC and Reuse  $\alpha$  closely overlap with each other (Fig. 10(a)). This shows that after performing power control over  $F_m^i$  subchannels, the effect of co-channels interference is nullified for UEs belonging to  $\mathcal{U}_m^i$ . For remaining MUEs ( $\mathcal{U}_m^r$ ), some deterioration in received bitrate is acceptable for HCPC technique. Resultantly, we see lower spectral efficiency of MUEs for HCPC compared to OSPA in Fig. 10(b).

Fig. 10 (c) illustrates the CDF of spectral efficiency of FUEs. It can be seen that there is a significant improvement in spectral efficiency of FUEs for Reuse  $\alpha$  compared to Reuse 1. This is the result of reduced co-channel interference from MBS to FUEs. However, availability of fewer subchannels for FUEs diminishes the FAP throughput drastically as can be seen in Fig. 12. OSPA technique shows significant improvement over Reuse 1 and Reuse  $\alpha$  techniques. This improvement is obtained due to optimal power distribution over  $F_m$  subchannels. Acquired results show that values of power factors for these subchannels vary from 0.27 to as high as 3.2. Finally, HCPC further improves FUEs' spectral efficiency by allowing FAPs to transmit at even higher power to their FUEs whilst satisfying MUEs' rate-loss constraint.



(a) ECR vs. REB for Max RSRP+Bias

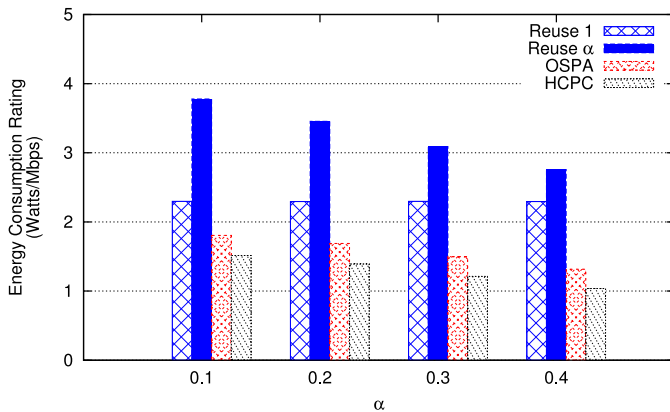
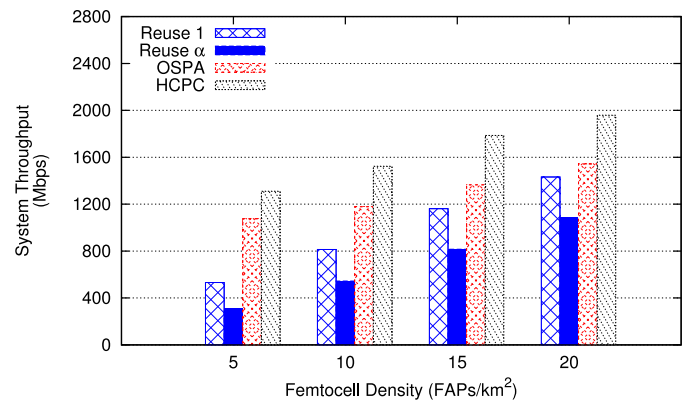
(b) ECR vs.  $\alpha$  for  $E[\hat{B}]$ 

Fig. 14. Energy efficiency.

We now compare the throughput and energy efficiency performance of Max RSRP + Bias and  $E[\hat{B}]$  schemes. We present the results for these two schemes only because in our previous work [14], Max RSRP + Bias and  $E[\hat{B}]$  have shown to outperform Max RSRP and  $E[B]$ , respectively. Additionally, results presented in Figs. 6 and 7 conclude that  $E[\hat{B}]$  scheme performs the best in terms of UE offloading, FAP throughput, and MBS energy consumption.

For Max RSRP + Bias scheme, the cell selection decision depends only on the REB. However, after cell selection, the bitrates of UEs are affected by the bandwidth availability in their target BSs. Hence, we analyse the performance of Max RSRP + Bias scheme for different spectrum allocation techniques by varying REB. The value of  $\alpha$  is taken to be 0.4 when Max RSRP + Bias scheme is used in combination with Reuse  $\alpha$ , OSPA, and HCPC techniques. Similarly, for  $E[\hat{B}]$  scheme, the cell selection decision depends only on the received bitrate or in turn the bandwidth availability at different BSs. For  $E[\hat{B}]$  scheme, REB has no effect on user association, and hence, the performance of different spectrum allocation techniques is studied by varying  $\alpha$ .

Fig. 11 (a) and 11(b) represent the MBS throughput for Max RSRP + Bias and  $E[\hat{B}]$  scheme, respectively. For Max RSRP + Bias, the MBS throughput decreases with increasing REB (Fig. 11(a)). This is due to the fact that, as REB increases, more users get offloaded to FAPs. This consequently results in a lower MBS throughput for all spectrum allocation techniques. A similar trend is observed for  $E[\hat{B}]$  scheme where reduction in MBS throughput is observed with an increase in  $\alpha$  for Reuse  $\alpha$ , OSPA, and HCPC techniques. This is due to the fact that, as  $\alpha$  increases, the bandwidth availability at FAPs increases. This, in turn, increases UEs association to FAPs, lowering



(a) System Throughput vs. FAP Density for Max RSRP+Bias

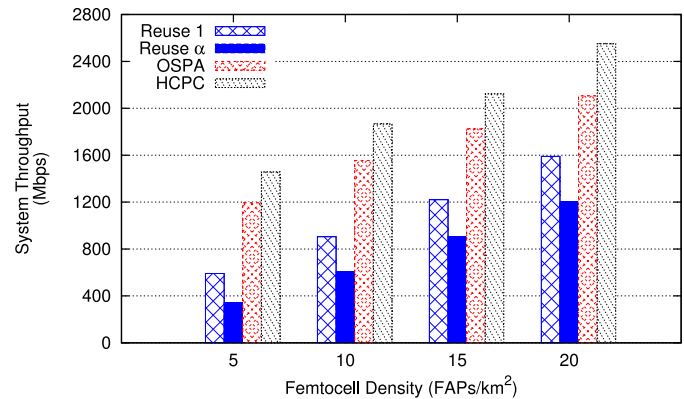
(b) System Throughput vs. FAP Density for  $E[\hat{B}]$ 

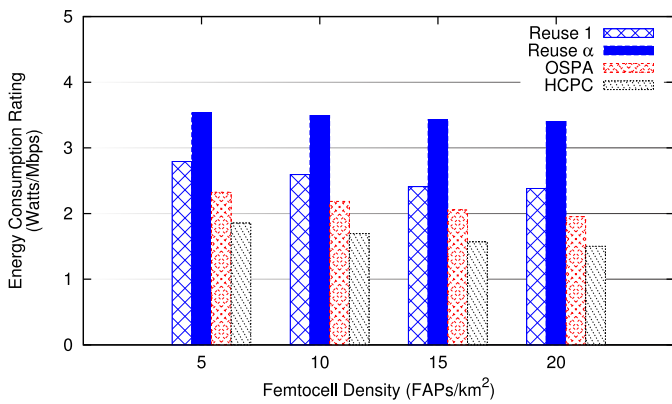
Fig. 15. Effect of FAP density on system throughput.

MBS throughput. For both cell selection schemes, the HCPC technique performs the worst as it reuses the macrocell spectrum for FUEs consequently deteriorating the throughput of MUEs due to increased interference.

Fig. 12 shows FAP throughput for Max RSRP + Bias and  $E[\hat{B}]$  schemes. For Max RSRP + Bias, the FAP throughput keeps increasing with increase in REB for all spectrum allocation techniques (Fig. 12(a)). A similar trend is observed for  $E[\hat{B}]$  scheme where improvement in FAP throughput is observed with an increase in  $\alpha$  (Fig. 12(b)). For both cell selection schemes, the maximum throughput is observed for HCPC technique due to reuse of macrocell spectrum for femtocell UEs. Note that, when  $E[\hat{B}]$  is used with Reuse 1 technique, the MBS and FAP throughput remain fixed for different values of  $\alpha$  as cell selection and spectrum allocation for UEs remain unchanged.

Fig. 13 represents the total system throughput (MBS + FAP) for Max RSRP + Bias and  $E[\hat{B}]$  schemes. As expected, HCPC performs the best in term of total system throughput for both cell selection schemes. Additionally,  $E[\hat{B}]$  scheme has shown to outperform Max RSRP + Bias scheme in terms of system throughput because it assigns UEs to BSs with an objective to maximize their bitrate. On an average,  $E[\hat{B}]$  has shown to improve the FAP throughput by 30–35% compared to Max RSRP + Bias scheme (Fig. 7). When HCPC is used with  $E[\hat{B}]$  scheme, higher transmit power over rate-loss protected subchannels ( $F_m^r$ ) results in an additional 20–26% improvement in FAP throughput compared to OSPA (Fig. 13(b)).

Fig. 14 makes it clear that HCPC technique is optimal in terms of energy efficiency too. For both cell selection schemes, HCPC has the least ECR compared to Reuse 1, Reuse  $\alpha$  and OSPA. This is a



(a) ECR vs. FAP Density for Max RSRP+Bias

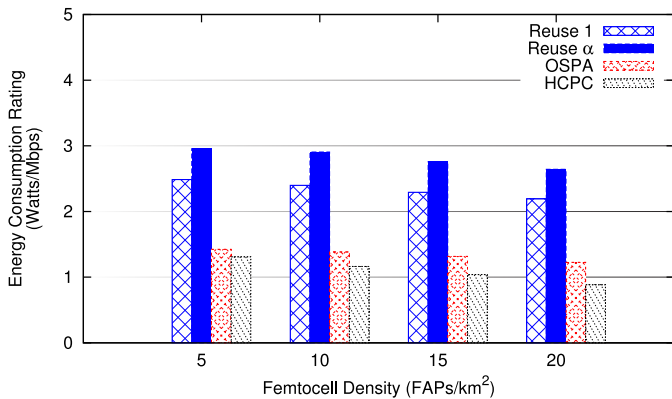
(b) ECR vs. FAP Density for  $E[\hat{B}]$ 

Fig. 16. Effect of FAP density on ECR.

direct consequence of throughput maximization for FUEs and reduction in MBS energy consumption. Also, as REB and  $\alpha$  increase for Max RSRP + Bias and  $E[\hat{B}]$ , respectively, more users get offloaded from MBS to FAPs. This further increases FAP throughput and reduces MBS energy consumption, lowering ECR.

Finally, we analyse the effects of increasing FAP density on system throughput and ECR for both cell selection schemes. As expected, with an increase in FAP density, system throughput increases for both Max RSRP + Bias and  $E[\hat{B}]$  due to higher spectrum reuse and users offloading in FAPs (Fig. 15). The offloaded UEs in FAPs are benefited by higher bandwidth allocation, causing improvement in both FAP and system throughput. Similar improvement in ECR is also observed with an increase in FAP density (Fig. 16) for both cell selection schemes. Interestingly, here too,  $E[\hat{B}]$  scheme when used with HCPC technique performs the best among all cell selection and spectrum allocation combinations.

## 8. Conclusion

In this paper, we have proposed an energy efficient framework for user association and power allocation in femtocell assisted cellular networks. In order to improve the benefits of femtocell deployments, use of cell biasing and expected bitrate based user association is suggested. These schemes offload users from macrocells to femtocells, and consequently improve the femtocell resource utilization and reduce the macrocell energy consumption. Compared to existing cell selection schemes available in the literature, our proposed enhanced expected bitrate scheme has shown to improve throughput of femtocells by 30–35% approximately. Be-

sides protecting signal quality of macrocell users using interference constraint, a new criterion referred to as rate-loss constraint is also proposed. Additionally, an optimal power allocation strategy (HCPC) is devised to efficiently reuse macrocell spectrum in femtocell downlink. The HCPC technique, when used in combination with enhanced expected bitrate scheme, has resulted in an additional 20–26% improvement in throughput of femtocells. Simulation results have verified this improvement in system throughput and energy efficiency. Our suggested HCPC technique achieves the best performance in terms of both system throughput and energy efficiency while protecting macrocell users via interference and rate-loss constraints. Future work in this direction can consider limited femtocell backhaul capacity while performing cell selection and spectrum allocation.

## Acknowledgement

This research work was supported by the Department of Science and Technology (DST), New Delhi, India.

## References

- [1] LTE heterogeneous networks, 2012, White Paper, URL <http://www.qualcomm.com/media/documents/qualcomm-research-lte-heterogeneous-networks>.
- [2] Cisco visual networking index: Global mobile data traffic forecast update, 2011–2016, 2012, White Paper. URL [http://www.cisco.com/en/US/solutions/collateral/ns341/ns525/ns537/ns705/ns827/white\\_paper\\_c11-520862.html](http://www.cisco.com/en/US/solutions/collateral/ns341/ns525/ns537/ns705/ns827/white_paper_c11-520862.html)
- [3] V. Chandrasekhar, J. Andrews, A. Gatherer, Femtocell networks: a survey, *IEEE Commun. Mag.* 46 (9) (2008) 59–67.
- [4] D. Feng, C. Jiang, G. Lim, L.J. Cimini, G. Feng, G. Li, A survey of energy-efficient wireless communications, *IEEE Commun. Surv. Tutorials* 15 (1) (2013) 167–178.
- [5] J. Andrews, H. Claussen, M. Dohler, S. Rangan, M. Reed, Femtocells: past, present, and future, *IEEE J. Sel. Areas Commun.* 30 (3) (2012) 497–508.
- [6] A. Imran, E. Yaacoub, M.A. Imran, R. Tafazolli, Distributed load balancing through self organisation of cell size in cellular systems, in: *Proceedings of the IEEE International Symposium on Personal, Indoor and Mobile Radio Communications*, 2012, pp. 1114–1119.
- [7] Market drivers for urban small cells, 2014, White Paper. URL <http://scf.io/en/download.php?doc=086>
- [8] Enterprise small cells : Overview, 2014, White Paper. URL <http://scf.io/en/download.php?doc=102>
- [9] P. Tian, H. Tian, J. Zhu, L. Chen, X. She, An adaptive bias configuration strategy for range extension in LTE-advanced heterogeneous networks, in: *Proceedings of the IET International Conference on Communication Technology and Application*, 2011, pp. 336–340.
- [10] A. Bou Saleh, O. Bulacki, S. Redana, B. Raaf, J. Hamalainen, Enhancing LTE-advanced relay deployments via biasing in cell selection and handover decision, in: *Proceedings of the IEEE International Symposium on Personal Indoor and Mobile Radio Communications*, 2010, pp. 2277–2281.
- [11] D. Lopez-Perez, X. Chu, I. Guvenc, On the expanded region of picocells in heterogeneous networks, *IEEE J. Sel. Top. Signal Process.* 6 (3) (2012) 281–294.
- [12] K. Balachandran, J. Kang, K. Karakayali, K. Rege, Cell selection with downlink resource partitioning in heterogeneous networks, in: *Proceedings of the IEEE International Conference on Communications Workshops*, 2011.
- [13] J. Oh, Y. Han, Cell selection for range expansion with almost blank subframe in heterogeneous networks, in: *Proceedings of the IEEE International Symposium on Personal Indoor and Mobile Radio Communications*, 2012, pp. 653–657.
- [14] R. Thakur, S. Mishra, C.S.R. Murthy, A load-conscious cell selection scheme for femto-assisted cellular networks, in: *Proceedings of the IEEE 24th International Symposium on Personal Indoor and Mobile Radio Communications*, 2013, pp. 2378–2382.
- [15] R. Madan, J. Borran, A. Sampath, N. Bhushan, A. Khandekar, T. Ji, Cell association and interference coordination in heterogeneous LTE-a cellular networks, *IEEE J. Sel. Areas Commun.* 28 (9) (2010) 1479–1489.
- [16] K. Lee, S. Kim, S. Lee, J. Ma, Load balancing with transmission power control in femtocell networks, in: *Proceedings of the International Conference on Advanced Communication Technology*, 2011, pp. 519–522.
- [17] A. Morimoto, N. Miki, H. Ishii, D. Nishikawa, Investigation on transmission power control in heterogeneous network employing cell range expansion for LTE-advanced uplink, in: *Proceedings of the European Wireless Conference*, 2012, pp. 1–6.
- [18] D. Zhou, W. Song, Interference-controlled load sharing with femtocell relay for macrocells in cellular networks, in: *Proceedings of the IEEE Global Telecommunications Conference*, 2011, pp. 1–5.
- [19] I. Ashraf, H. Claussen, L. Ho, Distributed radio coverage optimization in enterprise femtocell networks, in: *Proceedings of the IEEE International Conference on Communications*, 2010, pp. 1–6.
- [20] D. Fooladivanda, C. Rosenberg, Joint resource allocation and user association for heterogeneous wireless cellular networks, *IEEE Trans. Wirel. Commun.* 12 (1) (2013) 248–257.

- [21] J. Zhang, W. Wang, X. Zhang, Y. Huang, Z. Su, Z. Liu, Base stations from current mobile cellular networks: measurement, spatial modeling and analysis, in: Proceedings of the IEEE Wireless Communications and Networking Conference Workshops, 2013, pp. 1–5.
- [22] I. Katzela, M. Naghshineh, Channel assignment schemes for cellular mobile telecommunication systems: a comprehensive survey, *IEEE Commun. Surv. Tutorials* 3 (2) (2000) 10–31.
- [23] R. Thakur, A. Sengupta, C.S.R. Murthy, Improving capacity and energy efficiency of femtocell based cellular network through cell biasing, in: Proceedings of the 11th International Symposium on Modeling and Optimization in Mobile, Ad Hoc and Wireless Networks, 2013, pp. 523–530.
- [24] I. Ashraf, F. Boccardi, L. Ho, SLEEP mode techniques for small cell deployments, *IEEE Commun. Mag.* 49 (8) (2011) 72–79.
- [25] O. Arnold, F. Richter, G. Fettweis, O. Blume, Power consumption modeling of different base station types in heterogeneous cellular networks, in: Proceedings of the Future Network and Mobile Summit, 2010, pp. 1–8.
- [26] X. Wang, A.V. Vasilakos, M. Chen, Y. Liu, T.T. Kwon, A survey of green mobile networks: opportunities and challenges, *ACM Mobile Networks Appl.* 17 (1) (2012) 4–20.
- [27] X. Kang, H. Garg, Y.-C. Liang, R. Zhang, Optimal power allocation for OFDM-based cognitive radio with new primary transmission protection criteria, *IEEE Trans. Wirel. Commun.* 9 (6) (2010) 2066–2075.
- [28] E.C. Cherry, A history of the theory of information, *Proc. IEE - Part III* 98 (55) (1951) 383–393.
- [29] I. Guvenc, Capacity and fairness analysis of heterogeneous networks with range expansion and interference coordination, *IEEE Commun. Lett.* 15 (10) (2011) 1084–1087.
- [30] Drive testing LTE, 2014, White Paper. URL [http://www.jdsu.com/ProductLiterature/drivetesting\\_lte\\_wp\\_nsd\\_tm\\_ae.pdf](http://www.jdsu.com/ProductLiterature/drivetesting_lte_wp_nsd_tm_ae.pdf)
- [31] S. Ahmadi, LTE-Advanced : A Practical Systems Approach to Understanding 3GPP LTE Releases 10 and 11 Radio Access Technologies, Academic Press Inc., 2013.
- [32] S. Strzyz, K. Pedersen, J. Lachowski, F. Frederiksen, Performance optimization of pico node deployment in LTE macro cells, in: Proceedings of the Future Network and Mobile Summit, 2011, pp. 1–9.
- [33] W. Yu, R. Lui, Dual methods for nonconvex spectrum optimization of multicarrier systems, *IEEE Trans. Commun.* 54 (7) (2006) 1310–1322.
- [34] D. Palomar, M. Chiang, A tutorial on decomposition methods for network utility maximization, *IEEE J. Sel. Areas Commun.* 24 (8) (2006) 1439–1451.
- [35] S. Boyd, L. Vandenberghe, *Convex Optimization*, Cambridge University Press, Cambridge, UK, 2004.
- [36] C. Suh, M. Ho, D. Tse, Downlink interference alignment, *IEEE Trans. Commun.* 59 (9) (2011) 2616–2626.